PHYSICAL REVIEW B VOLUME 39, NUMBER 1 1 JANUARY 1989

Diffusion of oxygen in superconducting $YBa_2Cu_3O_{7-\delta}$ ceramic oxides

K. N. Tu, N. C. Yeh, S. I. Park, and C. C. Tsuei
IBM Research Division, Thomas J. Watson Research Center, Yorktown Heights, New York 10598

(Received 14 July 1988; revised manuscript received 13 September 1988)

We have used *in situ* resistivity measurements to monitor the diffusion of oxygen in and out of the ceramic oxide $YBa_2Cu_3O_{7-\delta}$. The study of out-diffusion of oxygen was carried out by annealing the oxide in ambient helium at constant heating rates and at constant temperatures. The rate of out-diffusion of oxygen has been found to be independent of δ, and the resistivity changes linearly with time during isothermal anneals. Assuming that the rate of out-diffusion is surface reaction limited, we have determined a surface barrier of 1.7 eV. The study of in-diffusion of oxygen was performed by annealing the oxygen-deficient oxide ($\delta=0.38$) in ambient oxygen. The in-diffusion rate was found to depend strongly on δ; we have determined the activation energies of the process at $\delta=0.38$ and $\delta=0$ to be 0.5 eV and 1.3 eV, respectively. The diffusivity of oxygen for $\delta=0$ has been determined to be $D=0.035\exp(-1.3\ \mathrm{eV}/kT)\ \mathrm{cm}^2/\mathrm{sec}$. Combining the kinetic data and published structural information, we have examined a vacancy mechanism and a twinning mechanism for anisotropic diffusion of oxygen in the CuO layer between the BaO layers.

I. INTRODUCTION

Both normal-state conducting and superconducting properties of the oxide depend strongly on the oxygen concentration.[1-4] How the oxide superconducts is as yet unclear. An effective way to study the superconducting mechanism and properties of the oxide is to vary the oxygen concentration. How to control the oxygen concentration and in turn the variation of the conduction behavior in a systematic manner is an important issue. It means more than just varying the amount of δ in $YBa_2Cu_3O_{7-\delta}$, i.e., the oxygen deficiency, but also to have a clear picture of the distribution of δ in the oxide, which must include the ordering of oxygen vacancies as well as any spatial gradient or inhomogeneity of oxygen. The parameter δ can be varied by a moderate annealing, and the variation of oxygen concentration only occurs in the O(1) sites, i.e., in the CuO chains.[1,2,5] Denoting the stacking layers of $YBa_2Cu_3O_7$ along the c axis by the formula $CuO_2/Y/CuO_2/BaO/CuO/BaO$, we may reduce the problem of controlling δ to the understanding of the intercalation and rearrangement of oxygen atoms in the CuO layer, i.e., the layer between the two BaO layers. The driving force of the intercalation can be monitored by the partial pressure of oxygen in the annealing ambient, and the kinetic rate can be changed by changing the annealing temperature.[6-8] Hence, we can perform a systematic study of oxygen intercalation in the oxide by properly selecting the ambient and the temperature of annealing. In this paper we report the response of the oxide subjected to anneal in ambient He and O_2. The responses have been recorded by *in situ* resistivity measurement. The kinetic behavior, the diffusivity and mechanism of oxygen diffusion in the CuO layer, and the δ distribution as a function of annealing condition are discussed on the basis of the measurements.

II. EXPERIMENT

We prepared the oxide samples from a mixture of powders of Y_2O_3, BaO, and CuO. The correct proportion was mixed, pressed into disks, and sintered at 950 °C for 40 h in air. The samples were then cooled down to 750 °C and held for 20 h in flowing oxygen atmosphere and finally furnace cooled to room temperature in about 7 h. The as-prepared samples showed a room-temperature resistivity of 2 to $3\times10^{-3}\ \Omega\,\mathrm{cm}$ and a superconducting transition temperature about 91 K (zero resistivity) and were assumed to contain seven oxygen atoms per unit cell, i.e., $YBa_2Cu_3O_{7-\delta}$ with $\delta\simeq0$. The microstructure as observed by scanning electron microscopy showed a large number of interconnecting pores and an average grain size of about 10 μm. The samples were dry cut by a diamond saw into rectangular pieces of about $13\times5\times1\ \mathrm{mm}^3$ size for resistivity measurements. A typical piece weighed about 0.3 g using a balance with a microgram sensitivity. Hence, a weight loss of 0.01% of the piece can be determined accurately. We note that the weight change of the oxide from $YBa_2Cu_3O_7$ to $YBa_2Cu_3O_{6.5}$ is 1.2%, taking the molecular weight of the former to be 666.2 g/mol.

For *in situ* resistivity measurements, we used the Pt-13% Rh alloy wires of 20-mils diameter to contact the specimen which was placed on a ceramic pad. The contacts were tested before the *in situ* measurements for Ohmic behavior in both positive and negative applied voltages. During the measurement, the current was kept constant at 20 or 50 mA, the average applied voltage was measured every half minute (or every 0.5 °C change), and the polarity check was carried out for every data point. The current-voltage measurement, temperature control, and rate of heating were controlled by an IBM personal computer.

Annealings of the specimen were performed in a quartz tube furnace flooded with He gas purified by a spongy Ti filter kept at 900 °C. The ambient can be switched from He to O_2 (or air) and vice versa at atmospheric pressure during the annealing. Both isothermal and ramping (at constant heating rate) modes of annealing were used. Combining the annealing mode and ambient, we can perform four types of *in situ* resistivity measurements; isothermal in He, ramping in He, isothermal in O_2, and ramping in O_2. Furthermore, the design of the quartz tube furnace is such that it enables us to quench the sample from the annealing temperature to room temperature without changing the ambient.

In addition to the resistivity measurements, the samples were characterized by scanning electron microscopy for surface morphology and grain size, x-ray diffraction for crystal structure, and Rutherford backscattering spectroscopy for averaging composition profile and surface segregation of cations. Results of these complementary measurements will not be reported here.

III. RESULTS

A. Out-diffusion of oxygen

The solid curve in Fig. 1 shows resistivity changes of the oxide of $\delta=0$ ramped at a constant heating rate of 3 °C/min starting from room temperature up to 550 °C in He. A linear increase from room temperature to about 350 °C was observed with a temperature coefficient of resistivity of 6.5 $\mu\Omega$ cm/K. Above 350 °C, resistivity increased nonlinearly and the increase accelerated up to 675 °C (not shown) where it reached a value about three orders of magnitude higher than the room-temperature value; then it bent and started to decrease.

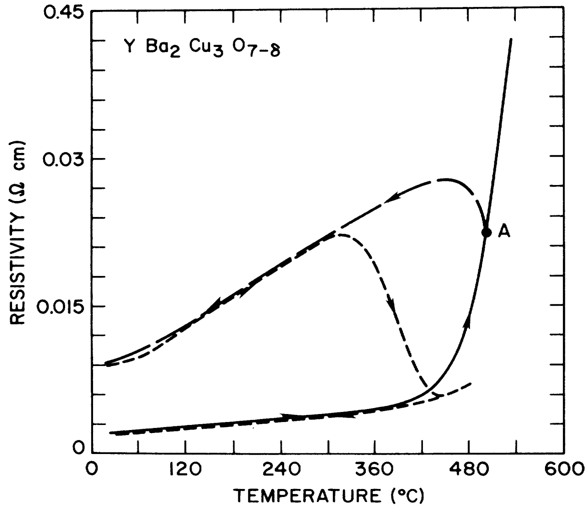

FIG. 1. *In situ* resistivity change of an oxide of $\delta=0$ upon annealing at a constant heating rate of 3 °C/min from room temperature to 600 °C in ambient helium is shown by the solid curve. If the heating was arrested at the point *A* and the power was turned off to let cooling start, the resistivity followed the long broken curve to a higher value at room temperature. If the oxygen-deficient sample was then annealed in ambient oxygen to replenish oxygen back into the sample, the resistivity followed the short broken curve to return to the very beginning.

If the heating was arrested at the point *A* shown in Fig. 1 and the power was turned off to let cooling start, the resistivity would follow the long broken curve to return to room temperature with a value higher than the initial one. During the cooling, the resistivity first increased with decreasing temperature because the temperature was still high enough for oxygen to diffuse out, then it reached a maximum, and decreased thereafter. Beyond 350 °C, it decreased monotonously with temperature and experienced a bend around 70 °C. At room temperature, we weighted the specimen to determine the weight loss and in turn the value of δ. Using a heating rate of 3 °C/min and furnace cooling, we obtained $\delta=0.38$ in our samples (weight loss $=0.92\%$) if we let the cooling start at 500 °C. It is clear that we can control δ by selecting the heating rate, the cooling rate, and the point *A* where the cooling starts. This is a reproducible process of controlling and varying δ.[9] In Fig. 1, the short broken curve which represents a process of diffusion of oxygen back into the oxide will be described later.

The question whether the measured resistivity changes come from the entire sample or rather from a skin layer of the sample is crucial for understanding the oxygen diffusion behavior. Since the weight loss and in turn the value of δ was measured for the entire sample, if the loss of oxygen were not from the entire sample but only from a skin layer, it would make the skin layer insulating ($\delta \simeq 1$) in the case of 0.92% weight loss; the insulating layer could be as thick as 0.2 mm in our samples of 1 mm in thickness. Since the resistivity of an oxide with such a thick insulating layer would be much higher than what we have measured, we conclude that the weight-loss measurement determines the oxygen deficiency in the entire sample.

The resistivity change shown in Fig. 1 indicates that oxygen diffuses out of the oxide in He at temperatures higher than 350 °C and beyond 500 °C the out-diffusion rate becomes extremely fast. To study the out-diffusion behavior, we have selected the temperature range of 350 to 450 °C for isothermal annealings. A typical isothermal annealing at 400 °C in He is shown by either one of the two solid curves in Fig. 2. We observed that except for the initial period, the resistivity increases linearly with time. To understand the out-diffusion behavior, we have to know the rate change of δ and the distribution of oxygen in the oxide during the isothermal annealings. Two experiments were performed in order to reveal them.

The first experiment performed was to check if the in-diffusion behaves the same as the out-diffusion. This was carried out by switching the ambient from He to O_2 during the annealing. The response of the resistivity to the ambient change was drastic. It dropped precipitously as shown in Fig. 2 by the vertical dotted curves, which indicates that the in-diffusion of oxygen was extremely fast and it quickly restored the resistivity back to its original value. It shows that the behaviors of out-diffusion and in-diffusion are asymmetrical; the latter is much faster. The asymmetrical behavior suggests that the out-diffusion process is not diffusion limited but rather surface reaction

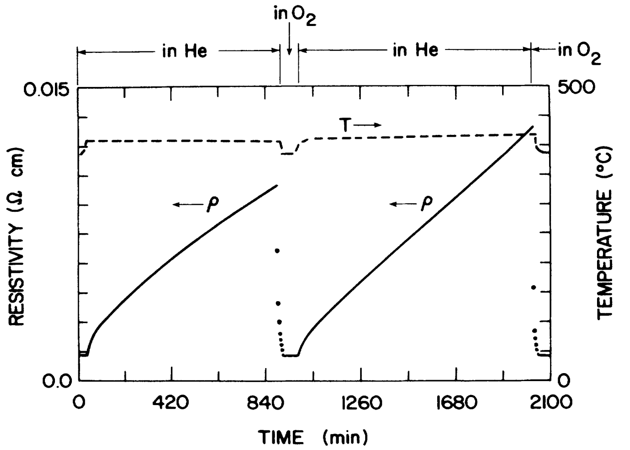

FIG. 2. A sequential annealing in He and O_2. The resistivity increases linearly and gradually in He (the solid curves) but drops instantaneously and precipitously in O_2 (the dotted curves). The dashed curve shows the temperature of annealing.

limited. Since it is not diffusion limited, the oxygen distribution in the oxide is expected to be homogeneous during the out-diffusion.

The second experiment was to arrest the isothermal annealing at a given time and to quench the sample to room temperature for weight-loss measurement. It enables us to correlate the changes of δ and resistivity at a fixed annealing temperature. The correlation is shown by the dashed curve in Fig. 3 for the annealing temperature of 425 °C; it is linear between δ and the increment in resistivity, $\Delta\rho$, for δ up to 0.4. We note that we have taken $\Delta\rho = \rho(\delta) - \rho_0$, where ρ_0 is the room-temperature resistivity extrapolated from the linear part of temperature dependence. Since the resistivity can be restored back to its original value and the weight loss can be regained by annealing the specimen in O_2, we conclude that the resistivity changes shown in Figs. 1 and 2 are due to the loss or gain of oxygen, and that oxygen concentration affects the majority carrier in the oxide. Also shown in Fig. 3 is the solid curve for the purpose of correlating the weight loss and δ.

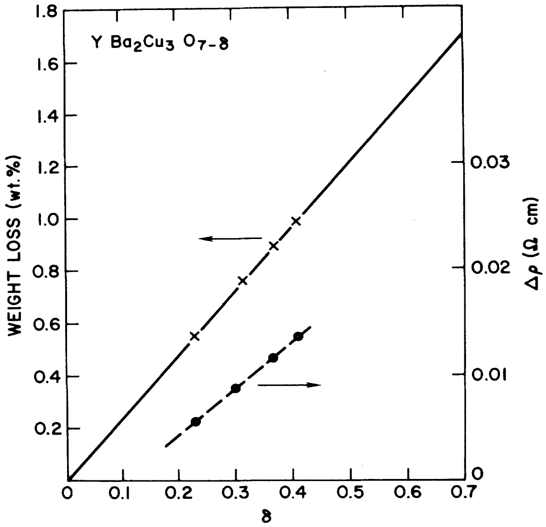

FIG. 3. The dashed curve shows the linear relation between the δ and the increment in resistivity, $\Delta\rho$, for δ up to 0.4. The solid curve shows the correlation between the weight loss and δ in the $YBa_2Cu_3O_{7-\delta}$ oxide.

To analyze the out-diffusion behavior of oxygen, we define that the amount of oxygen, $d\delta$, departing from the sample in a period, dt is

$$d\delta = AJ\,dt\ , \tag{1}$$

where A is the surface area, and J the oxygen flux normal to A. In general, for a surface-reaction-limited process, we express[7,10]

$$J = Kc'\ , \tag{2}$$

where c' is the oxygen concentration at the specimen (grain) surface which could be different from that within the grains; and K is the surface-reaction constant which monitors oxygen leaving the specimen (grain) surface. The observed fast in-diffusion of oxygen indicates that the diffusion of oxygen within the oxide in the temperature range being investigated is sufficiently fast that the rate-limiting step of oxygen flux leaving the specimen is to overcome a surface barrier. To determine the surface barrier, we first take into account the linear relation between the changes in resistivity and δ as shown in Fig. 3 and rewrite Eq. (1) into the following form: $d\Delta\rho/dt = BAKc'$, where B is a proportional constant. If we define $K = K_0\exp(-E/kT)$ where kT is the thermal energy and K_0 and E are the preexponential factor and activation energy of the surface-reaction constant, respectively, we have

$$\left[\frac{d\rho}{dt}\right]^{-1} = B_0\exp(E/kT)\ , \tag{3}$$

where B_0 is a proportional constant. Here we have replaced $\Delta\rho$ by ρ for simplicity. The activation energy can be determined by plotting $\ln(d\rho/dt)^{-1}$ vs $1/kT$, where $d\rho/dt$ at 400 °C, for example, is the slope of the solid curves shown in Fig. 2. The value of E was found to be 1.7 ± 0.1 eV on the basis of isothermal annealings carried out at 370, 390, 410, 425, and 440 °C as shown by the broken line in Fig. 4. It means that for oxygen to depart from the oxide it must overcome a surface barrier of 1.7 eV. We have observed that below 350 °C the thermal energy is insufficient to free a measurable amount of oxygen.

The temperature dependence of $d\rho/dt$ can also be measured from the slope of the curve of constant heating rate as shown in Fig. 1, provided that the heating rate is sufficiently slow.[11] The advantage of adopting this procedure is that it is a single measurement as compared to performing several isothermal annealings. For the constant heating rate annealing performed at temperatures above 350 °C in He as shown in Fig. 1, we have $\rho = \rho(T,t)$ and

$$\frac{d\rho}{dt} = \frac{\partial\rho}{\partial T}\frac{dT}{dt} + \frac{\partial\rho}{\partial t}\ , \tag{4}$$

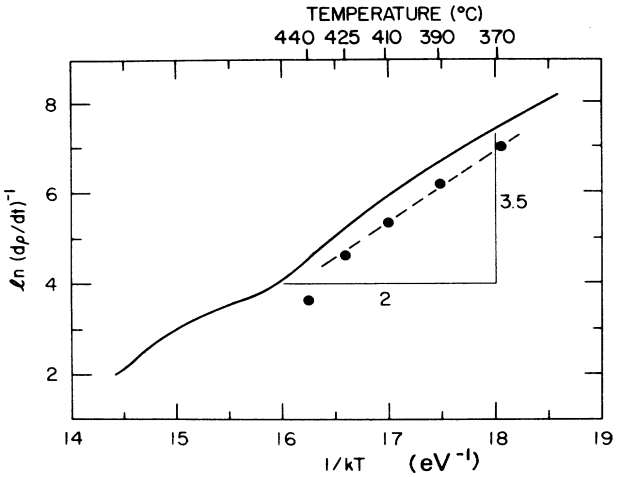

FIG. 4. The plot of $\ln(d\rho/dt)^{-1}$ vs $1/kT$, where the solid circles represent the data of isothermal annealings carried out at 370, 390, 410, 425, and 440 °C, and the solid curve from the constant heating rate of 0.5 °C/min from 350 to 530 °C.

where $\rho(T,t)$ is redefined as the resistivity after a subtraction of the linear temperature coefficient of resistivity. Equation (4) shows that the value of $d\rho/dt$ as a function of T can be determined by measuring, respectively, $\partial\rho/\partial T$ and $\partial\rho/\partial t$ from the data shown in Fig. 1 (where ρ, t, and T were measured simultaneously) with a subtraction of the linear temperature coefficient of resistivity. Figure 5 shows three constant heating rate annealings of 0.5, 1, and 10 °C/min in He of the oxide. We have found that the ρ vs T curves for a 0.3 °C/min and a 0.5 °C/min overlap each other closely, indicating that the latter is sufficiently slow. A plot of $\ln(d\rho/dt)^{-1}$ vs $1/kT$ from 350 to 530 °C of the curve 0.5 °C/min is given by the solid curve in Fig. 4. The average slope of the portion of the curve from 370 to 425 °C is 1.75 ± 0.1 eV, which is in very good agreement with the value of 1.7 ± 0.1 eV obtained from isothermal annealings. The transition of slope along the solid curve near 460 °C in Fig. 4 shows the orthorhombic-to-tetragonal phase transition of the oxide in ambient He. Above 460 °C, the slope is nearly the same as that of below, indicating that the activation energy for oxygen to depart from the tetragonal phase is about the same as that from the orthorhombic phase. However, we have observed a strong dependence of the orthorhombic-to-tetragonal transition temperature on the heating rate; the slower the heating rate, the lower the transition temperature. The latter was observed to be 440 and 510 °C for the 0.3 and 3 °C/min, respectively.

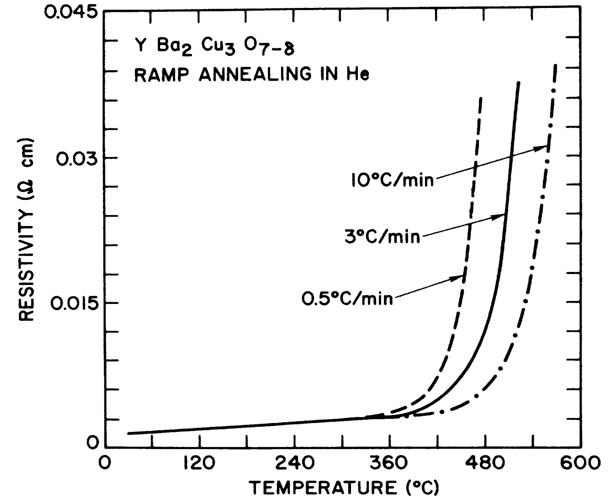

FIG. 5. Three resistivity curves of the oxide at constant heating rate annealing of 0.5, 3, and 10 °C/min in He.

B. In-diffusion of oxygen

In-diffusion of oxygen has been performed both at constant temperatures and at constant heating rates. We shall describe the latter first. We recall that in Fig. 1, as shown by the long broken curve, the specimen had a value of $\delta = 0.38$ at the end of the He annealing. We took the specimen and annealed it in ambient oxygen of 1 atmospheric pressure at a rate of 3 °C/min from room temperature to 500 °C, and the resulting resistivity change is shown by the short broken curve in Fig. 1. It started at the place where the annealing in He ended, followed the long broken curve in going up, but showed a more pronounced bend at around 70 °C. It reached a maximum around 319 °C and turned downward and decreased to a minimum around 443 °C. Beyond the minimum, the resistivity went up. In cooling, it followed the solid line to return to the very beginning of the annealing in He. After the oxygen annealing, δ was found to restore back to zero by weight-gain measurement, and T_c was determined to have the initial value of 91 K as shown in Fig. 6. We note

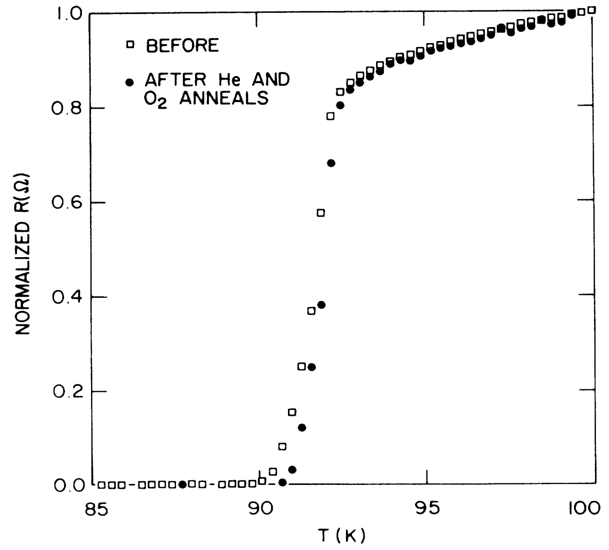

FIG. 6. Superconducting transition temperature measured by conduction of the oxide specimen before and after the cycling in He and O$_2$.

that the cycle of combining helium and oxygen annealings is repeatable and reproducible especially if a single specimen is used again and again.

Along the in-diffusion curve, the bend, the maximum, and the minimum in the resistivity are of interest. About the bend, we postulate that it is due to order-to-disorder transition of oxygen vacancies in the O(1) and O(5) sites in the CuO layer, and details of the transition will be reported elsewhere. The occurrence of the maximum shows the offset of the linear temperature dependence of the oxide by the increase of carriers as a result of in-diffusion. At the minimum, the oxide is saturated with oxygen, hence the resistivity goes up with temperature thereafter. We note both the minimum and the maximum are well defined and can be determined to within ± 1 °C.

The temperature at which the minimum resistivity occurs is a function of heating rate; the faster the heating rate, the higher the temperature, as shown in Fig. 7 where a plot of five oxygen anneal runs of 15, 10, 1, 0.3, and 0.1 °C/min is shown. Since a faster heating rate means a shorter time of annealing, a faster rate requires a higher temperature than that of a slower rate to diffuse the same amount of oxygen into the oxide. The temperature of the minimum therefore manifests the completion of in-diffusion in the oxide as δ approaches zero. Consequently, we can determine the activation energy of oxygen diffusion by measuring the dependence of the minimum on heating rate.

To consider the kinetics of in-diffusion in the CuO layer, we define J as the atomic flux, i.e., the number of diffusing oxygen atoms per cm^2 per sec; N_v as the number of O(1) oxygen atoms in the CuO layer per cm^3; and δ as the concentration (or fraction) of missing O(1) oxygen atoms in the CuO layer. In other words, δ is just a number varying from 0 to 1 as it is defined in $\mathrm{YBa_2Cu_3O_{7-\delta}}$. Now if we assume that the in-diffusion is a non-steady-state process, the total number of oxygen atoms diffused into the oxide per unit area over the entire period t_0 of in-diffusion is given by the following equation:[12]

$$N_v\delta=\int_0^{t_0} -(\nabla\cdot\mathbf{J})dt \,, \tag{5}$$

where $J=-D\partial(N_v\delta)/\partial x$ is the atomic flux, $D=D_0\times\exp(-E/kT)$ is the oxygen diffusivity in the oxide, and E is the activation energy of diffusion. By changing the base from time to temperature in Eq. (5) and by assuming a one-dimensional case since the grains in the sample are randomly oriented, we obtain

$$\delta=\int_{\mathrm{RT}}^{T_{\min}} D\left[\frac{\partial^2\delta}{\partial x^2}\right]\left[\frac{dt}{dT}\right]dT \,, \tag{6}$$

where RT is room temperature or a low temperature at which oxygen diffusion is negligible, and $T_{\min}$ is the temperature of the minimal resistivity. At constant heating rate, i.e., $dT/dt=$const, the solution of Eq. (6) can be obtained by following the thermal analysis of Kissinger[13] and Ozawa[14] to be

$$\delta\left[\frac{dT}{dt}\right]=\left[D_0\frac{\partial^2\delta}{\partial x^2}\right]\left[\frac{kT_{\min}^2}{E}\right]\exp(-E/kT_{\min})\,. \tag{7}$$

In obtaining Eq. (7), the two assumptions made are that E is a constant and that $\partial^2\delta/\partial x^2$ is a slowly varying function of temperature. These assumptions will be justified later. On the basis of Eq. (7), E can be measured by plotting $\ln[(dT/dt)/T_{\min}^2]$ vs $1/kT_{\min}$, or by plotting $\ln(dT/dt)$ vs $1/kT_{\min}$ since $T_{\min}$ does not vary much as compared to dT/dt. A plot of both, the latter in solid circles and the former in open circles from eight runs of heating rate of 14.7, 10.8, 6.5, 3, 1, 0.64, 0.3, and 0.1 °C/min, is shown in Fig. 8. The slopes of the lines which are least-squares fits to the data deliver activation energies of 1.35 and 1.23 eV, respectively, from the plot of $\ln(dT/dt)$ vs $1/kT_{\min}$ and the plot of $\ln[(dT/dt)/T_{\min}^2]$ vs $1/kT_{\min}$.[15–18] The uncer-

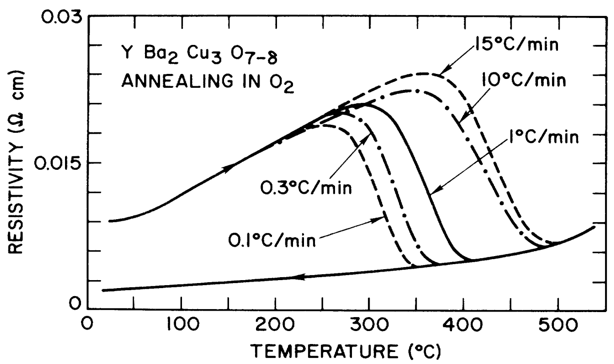

FIG. 7. A set of in-diffusion curves of oxygen-deficient samples ($\delta=0.4$) upon annealing in ambient O_2 at 15, 10, 1, 0.3, and 0.1 °C/min heating rate. The temperature of the maximum and the minimum resistivities increase with increasing heating rate.

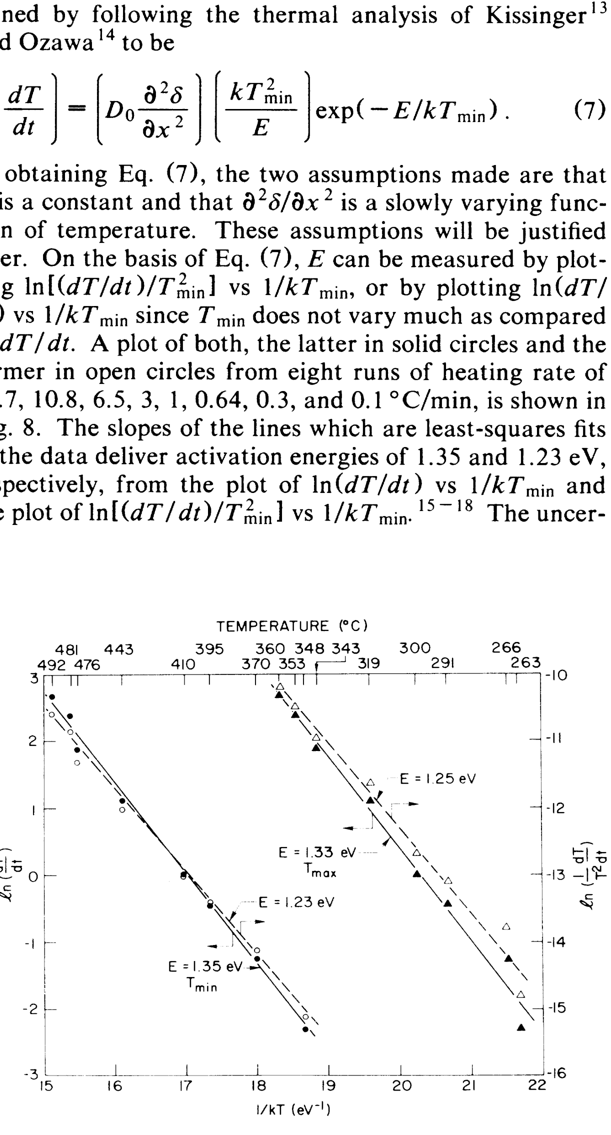

FIG. 8. The plots of $\ln(dT/dt)$ vs $1/kT_{\min}$ (the solid circles), $\ln[(dT/dt)/T_{\min}^2]$ vs $1/kT_{\min}$ (the open circles), $\ln(dT/dt)$ vs $1/kT_{\max}$ (the solid triangles), and $\ln[(dT/dt)/T_{\max}^2]$ vs $1/kT_{\max}$ (the open triangles) are shown, where $T_{\min}$ and $T_{\max}$ are the temperature of the minimum and the maximum resistivity, respectively, measured at the eight different heating rates given in the text. The activation energies obtained from the slope of the lines are indicated.

tainty of these measurements is ±0.1 eV, and the measured activation energy is insensitive to the initial value of δ as indicated by Eq. (7).

For comparison, we also show in Fig. 8 the plot of $\ln[(dT/dt)/T_{\max}^2]$ vs $1/kT_{\max}$ and the plot of $\ln(dT/dt)$ vs $1/kT_{\max}$ of the same eight runs, where $T_{\max}$ is the temperature of maximum resistivity, and the slopes yield activation energies of 1.33 and 1.25 eV, respectively, which are practically identical to those obtained from $T_{\min}$. It indicates that even in the early state of in-diffusion, a near-surface layer saturated with oxygen ($\delta=0$) has been developed and this layer limited the in-diffusion of oxygen with an activation energy of 1.33 eV (or 1.25 eV), so the assumption that E is constant throughout the process is justified. Although the layer thickens with temperature (or time), the oxygen concentration gradient in the layer does not vary much, so the other assumption that $\partial^2\delta/\partial x^2$ is a slowly varying function of temperature can also be justified. The formation of this near-surface layer is due to the in-diffusion of oxygen from room temperature to $T_{\min}$.

Having measured the activation energy, we shall next determine the preexponential factor of diffusion since they together constitute the diffusivity of oxygen in the oxide. Owing to the fact that the grains of the oxide become saturated with oxygen at $T_{\min}$, we can calculate the preexponential factor D_0 by the following equation:[9]

$$r^2=\int 4D\,dt=4D_0\left[\frac{dt}{dT}\right]\left[\frac{kT_{\min}^2}{E}\right]\exp\left[\frac{-E}{kT_{\min}}\right], \tag{8}$$

where r is the average radius of grains in the oxide. Taking $r=5$ μm and $E=1.3$ eV, we have obtained $D_0=0.035\pm0.005$ cm^2/sec based on the measured values of heating rates, dT/dt, and the corresponding temperatures of minimal resistivity, $T_{\min}$, as given in Table I. We note that while the heating rate varies by two orders of magnitude, the value of D_0 varies only slightly. Also, the value is neither unusually large nor unusually small as compared to the D_0 of other oxides.[19,20] Even if we change the numerical quantity "4" in Eq. (8) to other numbers, the order of magnitude of D_0 is still the same as we have determined.

Combining the preexponential factor and the activation energy, we have the expression of the diffusivity of oxygen in the oxide of $\delta=0$ to be

$$D=(0.035\pm0.005)\exp\left[\frac{-(1.3\pm0.1)\text{ eV}}{kT}\right]\text{ cm}^2/\text{sec}. \tag{9}$$

TABLE I. Preexponential factor of oxygen diffusion in $YBa_2Cu_3O_{7-\delta}$ ceramic oxides.

dT/dt (°C/min)	$T_{\min}$ (°C)	D_0 (cm^2/sec)
14.7	492	0.036
10.8	481	0.036
6.5	476	0.026
3	443	0.035
1	410	0.032
0.64	395	0.034
0.3	370	0.044
0.1	348	0.036

To determine if the diffusivity is physically reasonable, we demand that, for example, in the case of 1 °C/min annealing, oxygen atoms must be able to diffuse across the radius of grains in a period of minutes at $T_{\min}$. Now we evaluate $D=D_0\exp(-E/kT)$ at $T=410$°C and we obtained $D=9\times10^{-12}$ cm^2/sec. Such a value of D should allow oxygen atoms to diffuse a distance of the average radius of the grains in a period of 100 to 1000 sec. A similar agreement can also be shown for the other heating rates.

It is expected that the activation energy of oxygen diffusion in the CuO layer in the oxide may depend strongly on δ; the greater the δ, the lower the activation energy. However, we have shown in the last section that the near-surface layer or the shell formation will screen this δ-dependent behavior if we conduct in-diffusion of oxygen starting from a low temperature. To avoid the shell effect, the in-diffusion as a function of δ has to be carried out at high temperatures and the specimen must be kept in an inert environment until oxygen is introduced. Such experiments can be done if we follow the procedure shown in Fig. 9 by switching the annealing ambient from He to O_2 at a high temperature.[12] The dashed curve in Fig. 9(a) is a trace of the He-annealing curve given in Fig. 1 which has resulted in producing a specimen of $\delta=0.38$.

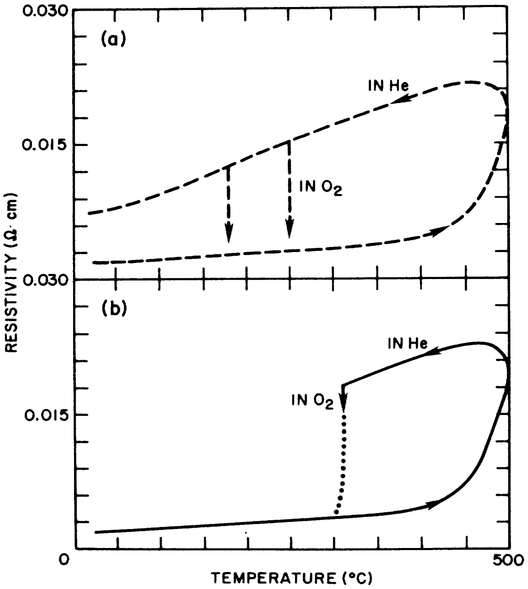

FIG. 9. (a) The dashed curve is a trace of the He-annealing curve given in Fig. 1 which has resulted in producing a specimen of $\delta=0.38$. The two arrows depict how the resistivity would change upon switching the ambient helium to oxygen and at the same time anneal isothermally at the two arbitrarily selected temperatures. (b) The curve records an actual anneal carried out at 310 °C of the specimen of $\delta=0.38$.

We recall that out-diffusion of oxygen will not occur below 350 °C in He. Therefore, if we cool the specimen in He to a temperature near and below 350 °C and switch the ambient to oxygen, the initial rate of in-diffusion will not be screened by a shell of $\delta=0$ since the shell formation has not yet occurred. Instead, it will be governed by the amount of excess oxygen vacancies in the oxide produced by the He anneal. In Fig. 9(a), the arrowed solid curves depict how the resistivity would change upon switching to ambient oxygen at the two selected annealing temperatures, and in Fig. 9(b) the data of an actual anneal carried out at 310 °C are shown. In Fig. 10, the temperature profile and resistivity change of the same anneal shown in Fig. 9(b) are replotted against the annealing time. We note that Figs. 9(b) and 10 show the same annealing situation except that the horizontal axis is different. We see in Fig. 10 that once the specimen was exposed to O_2, the resistivity dropped rapidly, yet it soon slowed down and became very sluggish at the end. We shall consider in the following the two extremes of the very rapid beginning and the sluggish end.

At the beginning of in-diffusion of oxygen in the sample of $\delta=0.38$, the oxide has a high concentration of oxygen empty sites in the CuO layers. The crystal lattice approaches the tetragonal symmetry where its a and b axes become nearly equal, and the c axis expands. Thus, the activation barrier for diffusion of oxygen in this case is much lower than that in $\delta=0$. The initial changes of resistivity at 360, 310, 260, and 210 °C are shown in Fig. 11. By plotting the slope of the initial resistivity drop at the four annealing temperatures in logarithmic scale against $1/kT$, we obtained the in-diffusion activation energy to be 0.48 ± 0.05 eV for $\delta=0.38$. The difference between the activation energies of 1.7 eV for out-diffusion and 0.48 eV for in-diffusion quantifies the asymmetrical behavior shown in Fig. 2. Using the latter value, it can be shown that a shell indeed forms readily at room temperature by the rapid diffusion of oxygen into an oxide which is oxygen deficient.

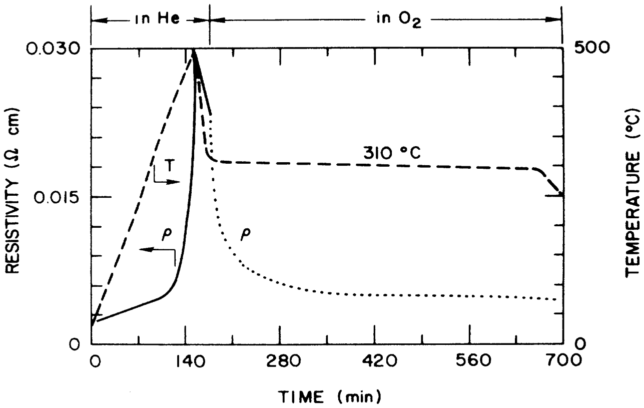

FIG. 10. The same set of data shown by the curve in Fig. 9(b) is replotted here using a different horizontal axis (time instead of temperature). Here, the broken curve shows the profile of annealing temperature starting from room temperature to 500 °C at a heating rate of 3 °C/min and followed by furnace cooling to 310 °C in He. Then the annealing temperature was kept at 310 °C and at the same time the ambient He was switched to O_2. The solid and the dotted curves show the corresponding resistivity changes in He and O_2, respectively. In O_2, the initial change of resistivity was rapid, but at the end the change was very sluggish.

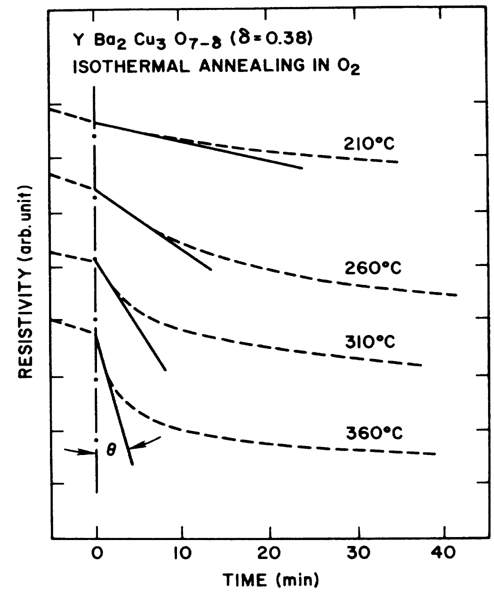

FIG. 11. The initial change of resistivity at constant temperature anneals carried out at 360, 310, 260, and 210 °C in ambient oxygen. The slope of the initial resistivity change is shown by the solid curves and the angle θ.

At the end of the annealing (where $\delta=0$), the diffusion of oxygen is much slower than that at the beginning. This is because at the end there are few excess vacancies in the O(1) sites in the CuO layers. Besides, the c axis contracts and the a and b axes are no longer equal. More important is the formation of a thick shell of $\delta=0$ which slows down the in-diffusion. By measuring the time needed to reduce a fixed amount of resistivity at the end of the annealing (or by measuring the total time needed at a constant temperature to restore the resistivity to the original value of $\delta=0$ since the initial period of large resistivity drop is relatively short), the activation energy of oxygen diffusion near $\delta=0$ has been determined to be about 1.1 to 1.2 eV. We expect it to be 1.3 eV and we find that the large uncertainty in this case is due to the difficulty in deciding the end point of the constant temperature annealing. In comparison, it is clear that the ramp annealing as shown in Fig. 7 is a better method for determining the activation energy of oxygen diffusion in oxides of $\delta=0$.

IV. DISCUSSION

We have measured three activation energies. They are the surface barrier of 1.7 eV to the out-diffusion of oxygen, the 1.3-eV activation energy of oxygen diffusion in oxides of $\delta=0$, and the 0.5-eV activation energy of oxygen diffusion into an oxide of initial $\delta=0.38$. We shall discuss in the following the physical meaning of these energies and begin with the mechanisms of oxygen diffusion in the oxide.

A. A vacancy mechanism of oxygen diffusion in the CuO layers

The in-diffusion and out-diffusion processes are nonconservative, i.e., empty O(1) lattice sites are occupied and created respectively by oxygen atoms in the processes. The oxygen diffusion must take place via lattice defects, because a conservative mechanism such as the direct exchange between two oxygen atoms will not result in a net flux of matter. Therefore, we shall consider a defect mechanism for diffusion of oxygen in the oxide.

Since vacant lattice sites are involved in the diffusion, the defects that mediate oxygen diffusion are vacancies rather than interstitials. This is also because it is hard to imagine how the latter can be restricted to take place in a plane only. Assuming a vacancy mechanism for oxygen diffusion, we analyze in the following the formation energy and motion energy of a vacancy in the oxygen sublattice in the CuO layer. We note that the sum of them is equal to 1.3 eV on the basis of our diffusion measurement, yet it is their partition that is being considered here.

To form an oxygen vacancy inside the oxide, we remove an oxygen atom from the O(1) lattice site and place it on a surface site which is an extension of the lattice. The surface is assumed to be exposed to vacuum so it is not covered by absorbed oxygen atoms, other elements, or molecules. In Fig. 12 we show an oxygen atom taking up a surface site at the end of an arbitrary *b* axis. On the other hand, to place the oxygen atom on a plane normal to the *a* axis, a surface step is needed and we will not consider it here. In forming the vacancy, there is a net change in bonding energy. To illustrate the change, we assume as given in the literature[21,22] that there exist there significant in-plane (in the CuO layer) pair interactions between oxygen atoms, i.e., V_1, V_2, V_3, as shown in Fig. 12, where V_1 and V_3 are repulsive and V_2 is attractive. The latter is mediated by Cu(1) and it is assumed that $V_1 > |V_2| \simeq V_3$. These pair-interaction energies have been utilized to generate the stable ground states of the two-dimensional structure of the CuO layer at $\delta = 0$ and $\delta = 0.5$. To form a vacancy, the change in pair interaction in the layer is

$$\Delta V = -V_2 - 2V_3 + V_{\text{Cu-O}} + V_{\text{Cu-Cu}} , \tag{10}$$

where $V_{\text{Cu-Cu}} > 0$ is the interaction energy between Cu(1) and Cu(1), and $V_{\text{Cu-O}} < 0$ the interaction energy between an O(1) oxygen atom and a Cu(1) copper atom at an open end, and we assume that $|V_2| < 2|V_{\text{Cu-O}}|$. In the right-hand side of Eq. (10), a negative sign is used whenever a pair is broken and a positive sign is used whenever a pair is formed. These assignments are to be kept in the subsequent equations. In placing an oxygen atom on the oxide surface as shown in Fig. 12(a), we have replaced a $V_{\text{Cu-O}}$ by a V_2 at the surface.

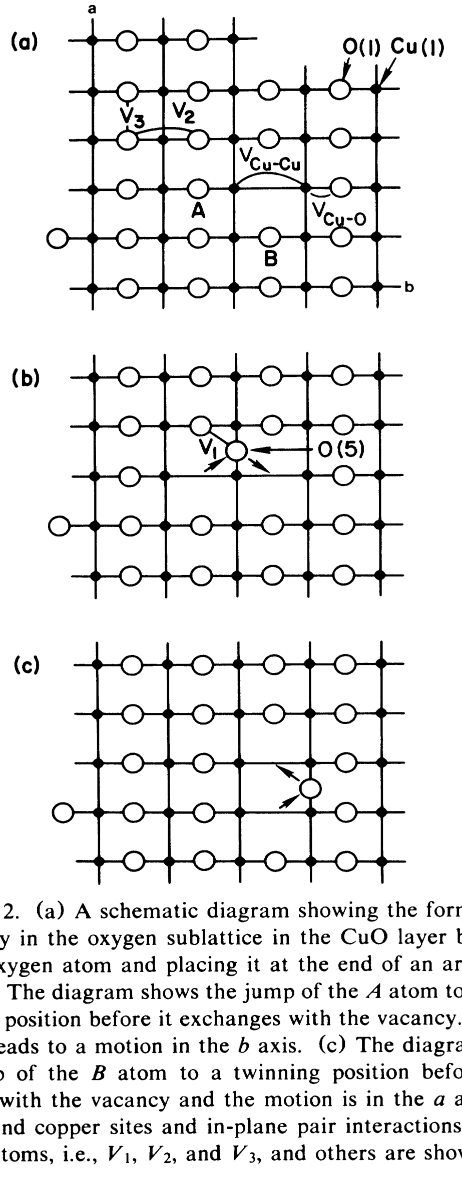

FIG. 12. (a) A schematic diagram showing the formation of a vacancy in the oxygen sublattice in the CuO layer by taking out an oxygen atom and placing it at the end of an arbitrary *b* axis. (b) The diagram shows the jump of the *A* atom to an O(5) twinning position before it exchanges with the vacancy. The exchange leads to a motion in the *b* axis. (c) The diagram shows the jump of the *B* atom to a twinning position before it exchanges with the vacancy and the motion is in the *a* axis. The oxygen and copper sites and in-plane pair interactions between oxygen atoms, i.e., V_1, V_2, and V_3, and others are shown in the diagrams.

The in-plane energy change given in Eq. (10), however, is only part of the energy spent in forming the vacancy. There must exist attractive out-of-plane interactions, $V_c < 0$, because in removing oxygen atoms from the O(1) sites the *c* axis expands. We then rewrite

$$\Delta V_f = -V_2 - 2V_3 + V_{\text{Cu-Cu}} + V_{\text{Cu-O}} - V_c , \tag{11}$$

where ΔV_f is the energy of formation of a vacancy. The effect of lattice relaxation around the vacancy has been ignored.

We note that the out-of-plane interaction is important because its attractive nature may play a role in relating the change in the superconducting transition temperature to the expansion along the *c* axis. The magnitude of V_c is unavailable and it is unclear whether it can be independently determined. On the other hand, it becomes known if the other terms in Eq. (11) can be measured. Hence, there is a need to measure the energy of formation of a vacancy and the in-plane pair interactions in oxides of $\delta=0$.

For an O(1) oxygen atom to diffuse by exchanging with a vacancy we assume that the oxygen atom must first move to a twinning position, the O(5) site, as shown in Figs. 12(b) or 12(c) before the exchange can take place. In the diagram shown in Fig. 12(b), the diffusion of the oxygen atom (or the vacancy) is along the b axis, and in Fig. 12(c) it is along the a axis. The twinning position as shown in Fig. 12(b) has a potential energy ($=2V_1-2V_3-V_2+V_{\text{Cu-Cu}}$) and the motion of the oxygen atom to the twinning position spends a kinetic energy (E_m). Here, we have ignored the out-of-plane interaction and we define their sum to be the energy of motion,

$$\Delta V_m=2V_1-2V_3-V_2+V_{\text{Cu-Cu}}+E_m\ . \tag{12}$$

Then we have the activation energy of oxygen diffusion in the CuO layer of $\delta=0$,

$$\Delta E=\Delta V_f+\Delta V_m\ . \tag{13}$$

It follows from Eqs. (11)-(13) that

$$1.3\text{ eV}=2V_1-2V_2-4V_3+2V_{\text{Cu-Cu}}+V_{\text{Cu-O}}-V_c+E_m\ . \tag{14}$$

There are seven unknowns in Eq. (14). We need six more independent measurements in order to solve them. The first three in-plane pair interactions could be determined from ordering kinetics. The values of $V_{\text{Cu-O}}$ and $V_{\text{Cu-Cu}}$ could be obtained from the formation energies of copper oxides and E_m from the relaxation process of quenched-in vacancies.

It is easy to show that the motion along the a axis as shown in Fig. 12(c) costs more energy than that along the b axis; the extra energy is $-V_2+V_3$. Hence, the diffusion of oxygen in the CuO layer is intrinsically anisotropic.

While we have considered in the above a vacancy mechanism of oxygen diffusion in the oxide of $\delta=0$, the mechanism must also operate in oxides of $\delta>0$. Since the latter has excess vacancies, the first question is whether the excess vacancies form an ordered structure or clusters. At low temperatures they tend to form ordered structures. Indeed, an order structure of $\delta=0.4$ has been observed by using electron diffraction.[23] We shall first consider the ordered structure and then the disordered structure. If we assume that oxygen vacancies prefer to line up along the b axis as a result of the attractive V_2 and repulsive V_3, the in-diffusion of an oxygen atom along the b axis needs only the energy of motion. Considering the oxygen atom at the twinning position shown in Fig. 13, we find the energy of motion to be

$$\Delta V_m^{\text{order}}=2V_1-2V_3+E_m\ . \tag{15}$$

We note that $\Delta V_m^{\text{order}}<\Delta V_m$, and therefore it is consistent with the assumption. The out-diffusion of an oxygen atom can be treated similarly.

For a disordered state, it is difficult to model the process and to evaluate the energy of motion since the distribution of the vacancies is not well defined. Instead, we approximate the energy of motion in the disordered state by the sum of

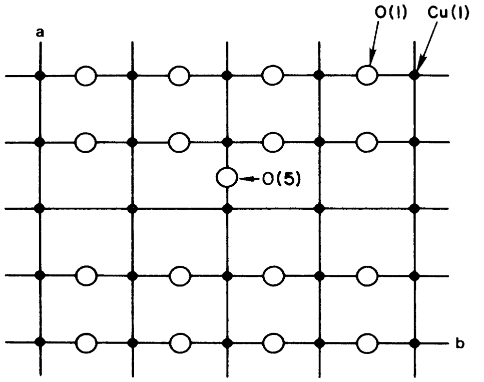

FIG. 13. A schematic diagram showing a row of ordered empty oxygen lattice sites along a b axis in the CuO layer. The diffusion of an oxygen atom along the axis is shown by taking a twinning position before jumping to a vacant site.

$$\Delta V_m^{\text{disorder}}=\Delta V_m^{\text{order}}+E_{d\text{-}o}\ , \tag{16}$$

where $E_{d\text{-}o}$ is the activation energy of the disorder-to-order transition in an oxide of $\delta>0$. The activation energy of 0.5 eV which we have measured from the rapid in-diffusion into the oxide of $\delta=0.38$ can be taken to be the energy of motion of oxygen in the disorder state. Since the measurements were performed at relatively high temperatures, the excess vacancies were randomly distributed.

B. A twinning mechanism of oxygen diffusion in the CuO layers

We consider here a mechanism of oxygen diffusion which does not led to a net flow of flux as in conservative reactions such as the orthorhombic-to-tetragonal transition at high temperatures for samples with $\delta=0$. Although a conservation reaction can be accomplished by the motion of a fixed number of vacancies, we consider here a process which allows two oxygen atoms to swap with each other without being mediated by a vacancy as discussed in the last section. In Fig. 14, the two oxygen atoms to be considered are labeled A and B. We first move A to a twinning position as shown in Fig. 14(a). For A to take the position of B, the latter must move away and there are three choices as shown in Figs. 14(b)-14(d). The one shown in Fig. 14(d) where A and B occupy opposite positions has the lowest change in energy;

$$\Delta V_{\text{twin}}=4V_1-2V_2-4V_3+4V_{\text{Cu-O}}+E_m\ . \tag{17}$$

A similar exchange between two oxygen atoms can also occur along the a axis as shown in Fig. 14(e); nevertheless, it is energetically less favorable than the one shown in Fig. 14(d). To decide whether the twinning mechanism can indeed take place in the oxide, we must compare its activation energy to that of the vacancy mechanism (1.3 eV), or to compare their components. Since the twinning mechanism does not involve breaking the bonds in the c direction, it could be a low-kinetic-energy process.

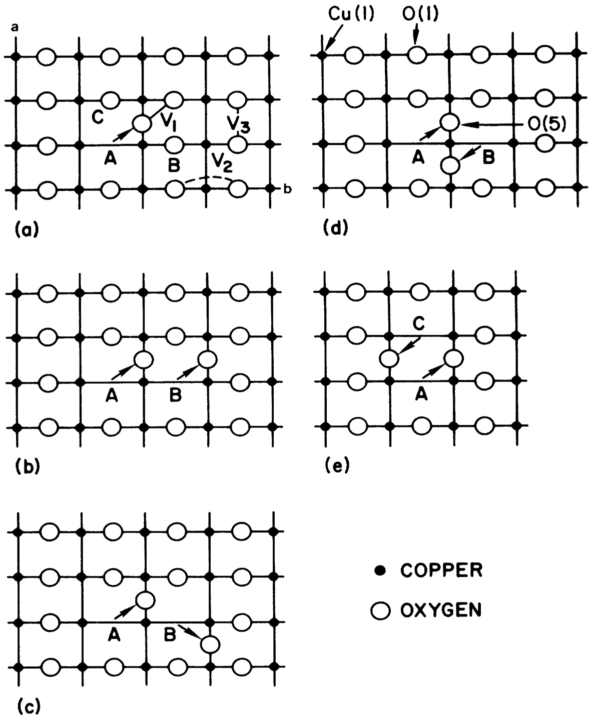

FIG. 14. A set of schematic diagrams shows the swap of two oxygen atoms in the CuO layer without involving a vacant oxygen lattice site. (a) The diagram shows the jump of the oxygen atom *A* to a twinning position. We assume the next jump is for the atom *B* to jump away so that the *A* can go to the vacant *B* site. (b) to (d) show the three possible jumps of *B*. The diagram in (d) shows the so-called twinning mechanism and has the lowest change in energy among the three. The diagram in (e) shows the exchange of two oxygen atoms along the *a* axis. It has a higher energy than the one shown in (d).

It has been shown that the magnitude of V_1 is about 0.2 to 0.22 eV.[24] Then, if we take E_m to be about 0.5 eV as given in the last section and discard the other terms (their sum is most likely a negative value, since the magnitude of V_2 and V_3 are assumed to be comparable), we have ΔV_{twin} close to 1.3 eV. Therefore, the activation energy of the twinning mechanism is indeed comparable to that of the vacancy mechanism. In other words, these two mechanisms could operate at the same time and enhance the rearrangement of oxygen atoms in the oxide. An experiment which can test this hypothesis is to mix ^{16}O and ^{18}O in the CuO layers in the oxide.

C. The surface barrier to out-diffusion of oxygen

The out-diffusion of oxygen in ambient He is rate limited by a surface barrier of 1.7 eV. The first question here is whether it is intrinsic to the oxide or it is rather due to an absorbed species or foreign phase. Because the out-diffusion anneals were carried out in a relatively high-temperature region, 370 to 440 °C, for a long time, 10 to 20 h, we expect that any absorbed species such as carbon would have been desorbed together with the departing oxygen and any foreign phase such as barium carbonate decomposed. In fact, the outgoing oxygen cleans the surfaces of the oxide as well as the grain boundaries. This is supported by electron spectroscopy for chemical analysis of a ceramic oxide annealed and analyzed *in situ* in vacuum of 10^{-11} torr. The spectrum showed no other phase except $YCu_2Ba_3O_{7-\delta}$ and also no other detectable impurities.[25]

In the previous section, we have considered the formation of a vacancy by removing an oxygen atom from a lattice site and placing it onto a surface site. Now if we remove two oxygen atoms from the lattice and place them on the surface and let them combine to form an oxygen molecule and then depart from the surface, the processes involved are surface diffusion, molecule formation, and desorption. However, there is a key difference between the formation of a vacancy and the formation of a departing oxygen molecule; the latter involves charge change in the oxide. Although charge neutrality in the oxide can be maintained by adjusting the valences of ions in the oxide, the charge change occurs when the oxygen molecule forms. It is clear that the activation energies needed for the surface diffusion, formation, and desorption of an oxygen molecule could be the surface barrier (or part of it) to the out-diffusion of oxygen.

The surface barrier is greater than the activation energy of oxygen diffusion in the oxide by 0.4 eV. Consequently, we expect a pileup of oxygen near the surface or grain boundaries before their departure. Also, the surface must be covered by oxygen atoms. In other words, inside the oxide δ is less than zero, yet near the surface δ is close to zero. It is even conceivable that the pileup could have increased the oxygen concentration in the CuO planes at the near-surface region from CuO to CuO_2 and this change in concentration could also be the source for the 0.4 eV increase in activation energy. The reason is that it requires a higher energy to form vacancies or to break bonds in CuO_2 since no loss of oxygen from the CuO_2 planes in the oxide was observed. It is unclear which of these processes dominates the surface barrier of the out-diffusion.

D. The shell formation during in-diffusion of oxygen

The shell formation in the oxide is characterized by an in-diffusion process which is two dimensional. For a single-crystal oxide which has a much larger dimension normal than parallel to the *c* axis, the anisotropic in-diffusion of oxygen will result in a shell formation. The shell of $\delta = 0$ is a good superconductor but the core is not if it is highly deficient in oxygen. The electrical and magnetic properties of such an inhomogeneous structure should be of interest. Also, it is conceivable that the superconducting current can be conducted via the shell or ring regions in a polycrystalline oxide sample containing otherwise a relative low amount of the superconducting phase.

V. CONCLUSIONS

(1) The out-diffusion of oxygen from ceramic $YBa_2Cu_3O_{7-\delta}$ oxides was performed by annealing the oxides in

ambient He at constant temperature from 300 to 440 °C and at constant heating rate (0.3 to 5 °C/min) from room temperature to 600 °C. The out-diffusion rate is independent of δ. The resistivity changes linearly with time. An activation energy of 1.7 eV has been measured by assuming that the out-diffusion rate is surface reaction limited.

(2) The in-diffusion was performed by annealing the oxygen-deficient oxides ($\delta = 0.4$) in ambient oxygen at constant temperatures from 210 to 360 °C and at constant heating rates (0.1 to 15 °C/min) from room temperature to 570 °C. The in-diffusion rate depends strongly on δ. The activation energies of the in-diffusion process at $\delta = 0.4$ and at $\delta = 0$ have been determined to be 0.5 and 1.3 eV, respectively. The oxygen diffusivity at $\delta = 0$ can be expressed as $D = 0.035 \exp(-1.3\ \text{eV}/kT)\ \text{cm}^2/\text{sec}$.

(3) Owing to the surface barrier and to the rapid oxygen diffusion within an oxide of $\delta > 0$, the out-diffusion results in a sample of $\delta > 0$ which is homogeneous in oxygen distribution. On the contrary, in-diffusion of oxygen into a sample of $\delta > 0$ ramping from room (or a low) temperature produces an inhomogeneous sample having a shell of $\delta = 0$. The shell which requires an activation energy of 1.3 eV for oxygen atoms to diffuse through becomes a barrier to the in-diffusing oxygen atoms.

(4) Both in-diffusion and out-diffusion processes are nonconservative reactions, i.e., empty oxygen lattice sites are occupied and created, respectively. A vacancy mechanism of oxygen diffusion has been proposed that the diffusion is mediated by vacancies in the oxygen sublattice. The formation and motion of a vacancy in the CuO layer have been discussed. Also the diffusion of oxygen atoms via a twinning mechanism has been proposed for conservative reactions such as the orthorhombic-to-tetragonal transition.

ACKNOWLEDGMENTS

The authors gratefully acknowledge J. Berosh for sample preparation, R. D. Thompson for the automation of resistivity measurement, and A. Levi for computer programming.

---

[1] J. D. Jorgensen, M. A. Beno, D. G. Hinks, L. Soderholm, K. J. Volin, R. L. Hitterman, J. D. Grace, I. K. Schuller, C. V. Serge, K. Zhang, and M. S. Kleefisch, Phys. Rev. B **36**, 3608 (1987).

[2] W. K. Kwok, G. B. Crabtree, A. Umezawa, B. W. Veal, J. D. Jorgensen, S.K. Malik, L. J. Nowicki, A. P. Paulikas, and L. Nunez, Phys. Rev. B **37**, 106 (1988).

[3] R. J. Cava, B. Batlogg, C. H. Chen, E. A. Rietman, S. M. Zahurak, and D. Werder, Phys. Rev. B **36**, 5719 (1987).

[4] S. I. Park, C. C. Tsuei, and K. N. Tu, Phys. Rev. B **37**, 2305 (1988).

[5] S. La Placa and R. Boehme (private communication).

[6] E. D. Specht, C. J. Sparks, A. G. Dhere, J. Bynestad, O. B. Cavin, D. M. Kroeger, and H. A. Oye, Phys. Rev. B **37**, 7426 (1988).

[7] K. N. Tu, S. I. Park, and C. C. Tsuei, Appl. Phys. Lett. **51**, 2158 (1987).

[8] P. P. Feitas and T. S. Plaskett, Phys. Rev. B **36**, 5723 (1987).

[9] N. C. Yeh, K. N. Tu, S. I. Park, and C. C. Tsuei, Phys. Rev. B **38**, 7087 (1988).

[10] U. Goesele and K. N. Tu, J. Appl. Phys. **53**, 3252 (1982).

[11] K. N. Tu, C. C. Tsuei, S. I. Park, and A. Levi, Phys. Rev. B **38**, 772 (1988).

[12] K. N. Tu, N. C. Yeh, S. I. Park, and C. C. Tsuei, Phys. Rev. B **38**, 5118 (1988).

[13] H. E. Kissinger, Anal. Chem. **29**, 1702 (1957).

[14] T. Ozawa, J. Thermal Analysis **2**, 301 (1970).

[15] D. S. Ginley, P. J. Nigrey, E. L. Venturini, B. Morosin, and J. F. Kwak, J. Mater. Res. **2**, 732 (1987).

[16] T. E. Evetts, R. E. Somekh, M. G. Blamire, Z. H. Barber, K. Butler, J. H. James, G. W. Morris, E. J. Tomlinson, A. P. Schwarzenberger, and W. M. Stobbs, in *Proceedings of the Symposia of the 1987 Spring Meeting of the Materials Research Society,* edited by D. U. Gubser and M. Schluter (Materials Research Society, Pittsburgh, 1987), p. 227.

[17] I. Haller, M. W. Shafer, R. Figat, and D. B. Goland, in *Proceedings of IUPAC Symposium on the Chemistry of Oxide Superconductors,* edited by C. N. R. Rao (Blackwell, Oxford, 1988), p. 93.

[18] J. L. Routbort, S. J. Rothman, L. J. Nowicki, and K. C. Goretta, in Proceedings of AUSTCERAM 88, International Conference on Ceramics, Sidney, Australia, 1988 (unpublished).

[19] Hj. Matzke, in *Nonstoichiometric Oxides,* edited by O. Toft Sorensen (Academic, New York, 1981), Chap. 4.

[20] A. S. Nowick, in *Diffusion in Crystalline Solids,* edited by G. E. Murch and A. S. Norwick (Academic, Orlando, 1984), Chap. 3.

[21] L. T. Wille and D. de Fontaine, Phys. Rev. B **37**, 2227 (1988).

[22] L. T. Wille, A. Berera, and D. de Fontaine, Phys. Rev. Lett. **60**, 1065 (1988).

[23] D. J. Werder, C. H. Chen, R. J. Cava, and B. Batlogg, Phys. Rev. B **37**, 231 (1988).

[24] H. Bakker, D. O. Welch, and O. W. Lazareth, Jr., Solid State Commun. **64**, 237 (1987).

[25] A. Schrott (private communication).